

PREVAILING DUST STORMS OVER THE HELLAS BASIN ON MARS AROUND SOUTHERN SPRING EQUINOX

K. C. Chow, K. L. Chan, *Space Science Institute, Macau University of Science and Technology, Block A, Avenida Wai Long, Taipa, Macau, China (kcchow@must.edu.mo)*

Introduction:

Dust storms can be commonly observed over the Hellas Basin of Mars, as reported in some literatures (e.g. Martin and Zurek [1993], Wang et al. [2015]). Incidentally, a number of observational studies (e.g. Cantor [2007]) suggest that the severe global dust storm occurred on Mars in 2001 was initiated at the Hellas Basin around the period of southern spring equinox (Ls 180°). The occurrence of dust storms over the Hellas Basin around this equinox period has been simulated in some modeling studies with general circulation model (e.g. Newman et al. [2002] and Basu et al. [2006]). These so-called Hellas storms could last for few days and usually initiated at the south or southwest edge region of the basin. At present, why the Hellas storms usually initiated and active mainly in this particular period is still an unanswered question. The present study is to address this question with a numerical model.

Configuration of Numerical Model:

A general circulation model MARSWRF has been used to simulate the Martian climate. This model is basically the Mars version of the PlanetWRF model (Richardson et al. 2007) developed on the basis of the National Center for Atmospheric Research (NCAR) Weather Research and Forecasting (WRF) model for Earth. It has been illustrated in Richardson et al. 2007) that the MARSWRF is capable of simulating the large-scale general circulation and temperature field on Mars. In this study, the global domain of the MASWRF model has 36 x 72 grid points (horizontal resolution ~ 5 degree or 300 km). There are 52 vertical sigma levels, and the model top is set at about 0.0057 Pa. The model has a specific radiation scheme for short wave and long wave, which has considered the heating/cooling effects of dusts and CO₂. The PBL scheme and physical parameterization are the usual schemes in WRF for Earth.

The model also includes some physical process parameterizations specific to Mars, such as the carbon dioxide cycle and the dust cycle. The parameterization of the water cycle is not included in the model.

The parameterization of the dust process in the model includes an interactive scheme and a dust devil scheme similar to that in Newman et al. (2002) and

Basu et al. (2006). The interactive scheme is similar to those dust models on Earth, in which the emission of dust is proportional to the surface wind stress. Dust emission occurs over the surface when the local surface stress exceeds a particular threshold value (constant value 0.042 N m⁻²). The suspended dust may change the atmospheric radiation and so the circulation. The process of dust devils is parameterized to provide the background dust field, with amount mainly depending on the surface temperature.

The model was run for eleven years. Each started at the time of northern spring equinox (Ls 0°). The first year is considered as the spin-up time. Therefore, only ten years simulation results will be considered and their ensemble mean is considered as the climatology of the model results.

Results and Discussion:

To compare with the modelling results, data of column dust optical has been obtained from the server of the Laboratoire de Météorologie Dynamique du CNRS (LMD, at http://www-mars.lmd.jussieu.fr/mars/dust_climatology/index.html). These are re-constructed data by Montabone et al. (2015, M2015 hereafter) based on the Thermal Emission Spectrometer (TES) data and the Thermal Emission Imaging System (THEMIS) data. These gridded, daily-mean data cover Martian years (MY) 24 to 31. As in M2015, we used the six Martian years without global or large regional dust storms (MY24, 26, 27, 29, 30, and 31) to obtain the climatology of dust optical depth.

From the time series of the M2015 climatological data averaged over the Hellas basin (blue crosses in Fig. 1), we can see that there is a prominent episode of column dust optical depth around Ls 170°, close to the southern spring equinox (Ls 180°). It is worth mentioning that although there is another stronger episode around Ls 240°, the significantly large dust optical depth during this period is not limited to the Hellas Basin, but is a general feature in the southern hemisphere that is basically associated with the significant increase in surface temperature during the southern summer season. Also, the third episode around Ls 320° is not limited to the region of the Hellas Basin. This episode in dust may be associated with the condensational flow of CO₂.

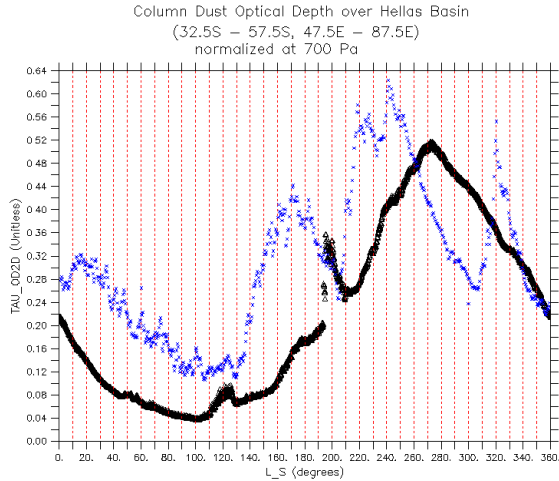


Figure 1. Time series of column dust optical depth at $9.3 \mu\text{m}$ (normalized to surface level 700 Pa) averaged over the Hellas Basin region (32.5°S to 57.5°S , 47.5°E to 87.5°E). One curve (blue crosses) is from the re-constructed observational data of LMD (Montabone et al. 2015) averaged for six Martian years without global-scale dust storm. Another curve (black triangles) is from the ten-year averaged model results.

In the ten years model simulations, the occurrence of Hellas storms can be found in nine years in different periods between 180°Ls and 200°Ls . The storms last for a period between 2 to 5 days. The occurrence of Hellas storms can be seen from the corresponding time series of model climatology (the episode around $\text{Ls } 200^\circ$ in Fig. 1). The model could also reproduce the maximum in dust optical depth near the southern summer solstice. However, the model cannot reproduce the third episode around $\text{Ls } 320^\circ$.

The spatial distribution of the column dust optical depth in the episode period near the southern spring equinox is shown in Fig. 2. The M2015 data and model results both show a significant dust distribution in the Hellas Basin. It is worth-noting that a significant dust distribution can also be found near the Argyre Basin from the M2015 data, but cannot be reproduced by the model simulations.

Indicated by the idealized numerical study of Siili et al. (1999), it can be realized that the episode of dust in the Hellas Basin near the period of southern spring equinox is likely related to the down slope flow associated with the sublimation of CO_2 ice in the ice cap edge region. The southern spring equinox is the period when the CO_2 ice starts to sublimate.

The model results in Fig. 3 suggest that the increase in down slope flow and so the increase in surface stress over the southern edge of the Hellas Basin during the period of southern spring equinox may be associated with the strong surface temperature difference between the southern edge of the basin and the

ice covered surface in the south. Well before the southern spring equinox ($< \text{Ls } 120^\circ$), the southern edge is still covered by ice (Fig. 4) and so the temperature difference is small. When solar radiation is further increasing in the south, the CO_2 ice over the southern edge starts to sublimate and so the temperature difference increases significantly. This is accompanied with the sharp increasing in surface stress over the southern edge, despite the decreasing in surface air density during this period (Fig. 4). The increasing in temperature difference and stress stops around $\text{Ls } 200^\circ$. Beyond this time the ice in the south of the southern edge also sublimates and so the temperature difference decreases significantly, and so the surface stress over the southern edge.

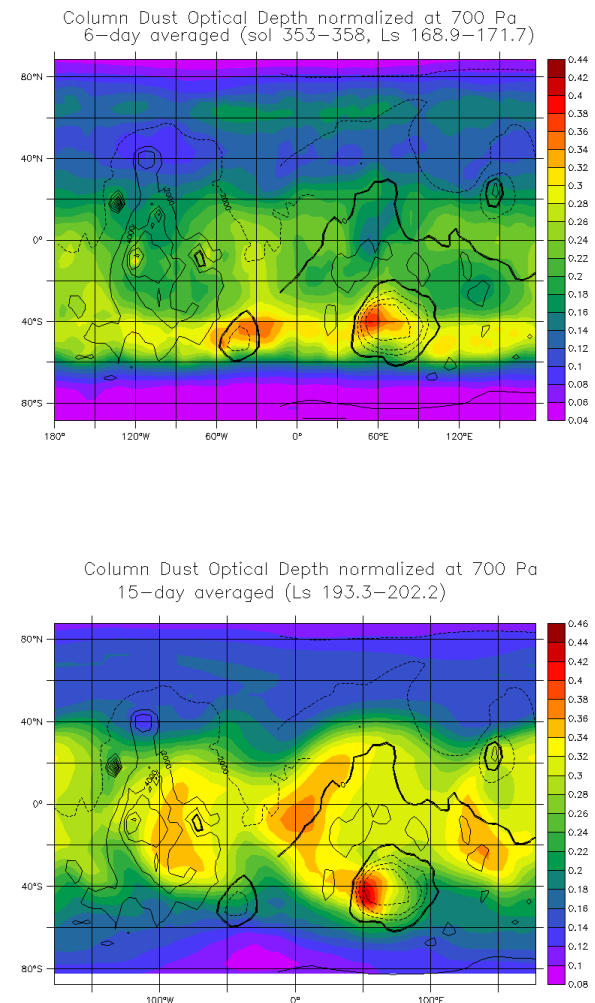


Figure 2. Column dust optical depth at $9.3 \mu\text{m}$ (normalized to surface level 700 Pa) averaged around the period of southern spring equinox. (Upper) Re-constructed observational data of LMD (climatology of six Martian years without global-scale dust storm) averaged for 6 days from $\text{Ls } 168.9^\circ$ to 171.7° . (Lower) Model results (ten-year climatology) averaged for 15 days from $\text{Ls } 193.3^\circ$ to 202.2° . Contours are topography with intervals 2000 m.

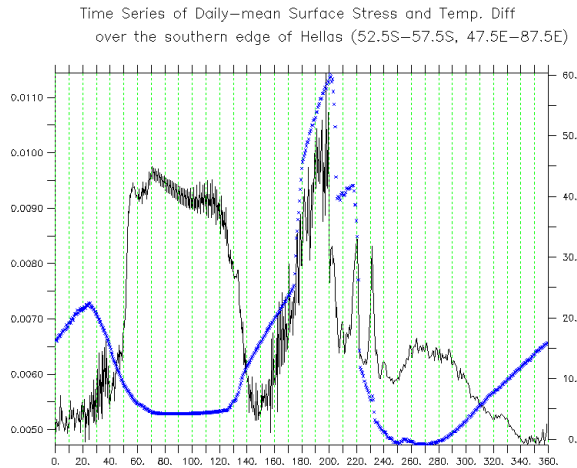


Figure 3. Time series of daily mean model results (ten-year climatology) over the southern edge region of the Hellas Basin (averaged 52.5°S to 57.5°S , 47.5°E to 87.5°E). Black curve shows surface stress (N m^{-2} , left axis) and the blue crosses show surface temperature difference (K) between the southern edge region and a region of the same area in the south (62.5°S to 67.5°S , 47.5°E to 87.5°E).

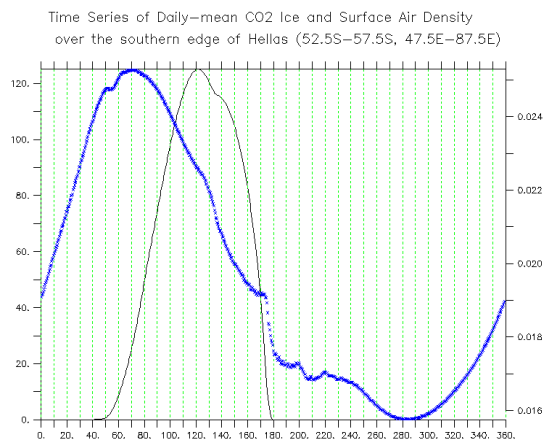


Figure 4. Time series of daily mean surface air density (kg m^{-3} , left axis) and surface carbon dioxide ice (kg m^{-2}) from model results (ten-year climatology) over the southern edge region of the Hellas Basin (averaged 52.5°S to 57.5°S , 47.5°E to 87.5°E).

Acknowledgement

This research is funded by the grants from the FDCT of Macau (grant no. 039/2013/A2 and 080/2015/A3).

References:

- Basu, S., J. Wilson, M. Richardson, A. Ingersoll (2006). Simulation of spontaneous and variable global dust storms with the GFDL Mars GCM, *J. Geophys. Res. (Planets)*, 111(E10), 9004, doi: 10.1029/2005JE002660.
- Cantor, B.A. (2007). MOC observations of the 2001 Mars planet-encircling dust storm. *Icarus*, 186, 60 - 96.
- Martin, L. J., R. W. Zurek (1993). An analysis of the history of dust activity on Mars *J. Geophys. Res.*, 98, 3221 - 3246.
- Montabone, L., Forget, F., Millour, E., et al. (2015). Eight-year climatology of dust optical depth on Mars, *Icarus*, 252, 65 - 95
- Newman, C. E., S. R. Lewis, P. L. Read, F. Forget (2002), Modeling the Martian dust cycle: 2. Multiannual radiatively active dust transport simulations, *J. Geophys. Res.*, 107(E12), 5124, doi:10.1029/2002JE001920.
- Richardson, M.I., Toigo, A.D., Newman, C.E. (2007). PlanetWRF: A general purpose, local to global numerical model for planetary atmospheric and climate dynamics, *J. Geophys. Res.* 112, 2006JE002825.
- Siili T., R. M. Haberle, J. R. Murphy, H. Savijarvi. (1999). Modelling of the combined late winter ice cap edge and slope winds in Mars' Hellas and Argyre regions, *Planetary and Space Sci.*, 47, 951-970.
- Wang, H., Richardson M.I. (2015). The origin, evolution, and trajectory of large dust storms on Mars during Mars years 24 - 30 (1999 - 2011). *Icarus* 251, 112-127.